INVESTIGATION OF THE STRUCTURE OF RADIATION DAMAGE IN LITHIUM-DIFFUSED SILICON

Final Report Covering Period
1 January 1970 through 5 October 1970

Rensselaer Polytechnic Institute
Troy, New York

INVESTIGATION OF THE STRUCTURE OF RADIATION DAMAGE IN LITHIUM-DIFFUSED SILICON

Final Report Covering Period
1 January 1970 through 5 October 1970

JPL Contract No. 952456

Prepared for:

National Aeronautics and Space Administration
Jet Propulsion Laboratory
4800 Oak Grove Drive
Pasadena, California 91103

Principal Investigator:

John C. Corelli
Nuclear Science Department
Rensselaer Polytechnic Institute

INVESTIGATION OF THE STRUCTURE OF RADIATION DAMAGE IN LITHIUM-DIFFUSED SILICON

Final Report Covering Period
1 January 1970 through 5 October 1970

John C. Corelli

JPL Contract No. 952456

Prepared For:

National Aeronautics and Space Administration
Jet Propulsion Laboratory
4800 Oak Grove Drive
Pasadena, California 91103

"This work performed for the Jet Propulsion Laboratory, California Institute of Technology, as sponsored by the National Aeronautics and Space Administration under contract NAS7-100"

Nuclear Science Department
Rensselaer Polytechnic Institute
Troy, New York 12181

TABLE OF CONTENTS

ABSTRACT

A brief description is given of instrumentation and methods used in the study of radiation damage in lithium-diffused Si. Infrared photoconductivity (1 to 10 microns) and infrared spectroscopy (1 to 50 microns) were used as the probes. The defects were induced in the material by 1.5MeV electrons with the sample temperature at 300°K during irradiation; one irradiation experiment was run at $\sim$110°K. No infrared active defect bands were induced by electrons of $E \lesssim 5$MeV up to radiation fluences of $3.3 \times 10^{17} e/cm^2$. All samples studied which have lithium concentrations in the range $9 \times 10^{15} cm^{-3}$ to $2 \times 10^{17} cm^{-3}$ exhibit sharp increases in resistance after heat treatment in the range 200° to 700°K. Dominant radiation-induced photoconductivity arises from levels at E_c-0.2, E_c-0.39, E_c-0.54, E_c-0.6, E_c-0.7, and E_c-0.8eV in oxygen-rich Si and at E_c-0.2, E_c-0.54, E_c-0.8, E_c-0.92, and E_c-1.0eV in oxygen-lean Si. The levels are found to disappear and in some cases shift with annealing in the 100° to 450°C temperature range. In all cases the spectrum is dominated by 3 or 4 energy levels after irradiation and after various anneals. Energy levels obtained by other workers using carrier concentration, minority carrier lifetime, and photoluminescence as the probes are compared to our measurements.

I) INTRODUCTION

The main emphasis of the research program was to make a study of the extrinsic photoconductivity (1 to 10 μ) and infrared absorption induced in silicon by $\sim$ 1.5 to 2.5 MeV electrons. The silicon was doped by lithium diffusion to concentrations of $\sim 10^{16}$ to 10^{17} Li atoms/cm^3 from starting material that was $\sim 10\,\Omega$-cm phosphorus-doped. The silicon was either oxygen-lean ($\lesssim 10^{16}$ oxygen/cm^3) float zone refined (FZ), or oxygen-rich ($\gtrsim 10^{17}$ oxygen/cm^3) grown by pulling from the melt in a quartz crucible (CG). The irradiations were performed with the sample kept at $\lesssim$ 300°K during bombardment with subsequent annealing to temperatures of $\sim$ 700°K. One irradiation was performed with the sample kept at a temperature of $\sim$ 100°K during bombardment with subsequent annealing to $\sim$ 250°K.

The primary purpose of this research was to investigate the effects of lithium on radiation-produced complexes which had long term stability ($\sim$ days to weeks) by examining the appearance of localized energy levels in the forbidden gap giving rise to extrinsic photoconductivity (PC). In addition, the infrared spectrum was measured (at 78°K) on samples after irradiation to obtain additional information on Li-associated defect bands which might be correlated with the localized defect energy states.

In the case of the infrared spectroscopy measurements, it is significant to point out that the relatively low fluences of $\sim$ 1.5 MeV electrons $\lesssim 8 \times 10^{17}$ e/cm^2 used in the experiments were never sufficient to produce detectable defect infrared bands. These results are consistent with our past research[1] on infrared spectroscopy studies on 50 MeV electron-irradiated Li-doped Si in which it was found that the sample must be exposed to fluences of

$\gtrsim 10^{18} e/cm^2$ in order to produce a sufficient number of infrared active defect centers. The scope and effort of the present program did not include a study of the damage induced by 50 MeV electrons.

The ultimate purpose of our research was to be the understanding of the basic processes operative in the radiation damage process in Li-doped Si, particularly as the processes relate to solar cell operation in a radiation environment. Moreover, it was anticipated that the results of our method of probing the defects might be compared to results obtained by workers using other probes such as luminescence, temperature dependence of carrier concentration, and carrier lifetime studies. A review of the reports of other workers has shown only a meager correlation because of factors such as lack of high temperature annealing data, different irradiation temperature, markedly different Li concentration in the sample, and different electron fluences to which the samples were exposed. In some cases little or no comparison can be made since results of other studies have just recently become available from programs started 2 1/2 years ago*.

---

* We recommend that a uniform procedure be followed for supplying Li-diffused samples to various research groups in that they should all come from a common source. This procedure would at least insure similar starting conditions. It is recognized that the probes used to study the defects by the various groups require different fluences due to sensitivity requirements of the measuring probe. However, it is our judgment that even with this disadvantage (unavoidable) comparison of results of various workers would be made easier. This factor should be given serious consideration in future programs.

The level of the effort spent on this program represents 1.0 man year made up of the principal investigator, a graduate student, and an undergraduate student assistant, all on a part time basis.

II) Experimental Methods

Details of the experimental methods used in our research program have been given in earlier reports[2,3] and most will not be repeated here. Our main purpose in this report will be to give in brief form, the salient features of the experimental methods and techniques used in the measurements.

A) Sample Preparation

The lithium was diffused into the silicon using a painting procedure in which a paste composed of dispersed lithium metal and 15 micron alumina mixed in mineral oil was applied to the surface of the sample. The nominal sample dimensions were 2 x 5 x 18 mm. The "painted sample" was given a 10 to 20 minute heat treatment at $\lesssim$ 450°C to cause the first in-diffusion of Li. The lithium concentration was monitored by four-point electrical resistivity measurements which are sensitive to the electrically active lithium atoms that introduce donors. Homogeneity of the Li (to within $\pm$ 5%) was accomplished by redistribution at $\lesssim$ 450°C for 1 to 10 hours depending upon the final lithium concentration desired. All heat treatments were made while the sample was in an inert gas atmosphere. We have routinely produced samples having lithium concentrations of $\sim 10^{15}$, $\sim 10^{16}$, and $\sim 10^{17} cm^{-3}$ from starting material of 10 Ω-cm P-doped Si both oxygen-lean and oxygen-rich.

In order to make the optical measurements, opposite faces of the sample are polished to a mirror-like finish using 15 micron alumina followed by $\approx$ 1 and 0.3 micron alumina polishes. Since two electrical contacts to the sample are needed to make photoconductivity measurements,

we use a gold alloying technique* in which gold doped to 1 or 2 atomic percent Sb is pressure bonded to the silicon at $\approx 380^{o}C$. The pressure is kept on the sample at $350^{o}C$ for approximately 5 minutes while the sample is in an inert atmosphere. Contacts made in this fashion were ohmic and non-rectifying at $78^{o}K$ and remained so even after irradiation.

B) Electron Irradiation

Most of the electron irradiation experiments were performed using a 1 - 3 MeV electron Van de Graff accelerator. The samples were kept at $\lesssim 300^{o}K$ during bombardment. Sample cooling was accomplished by using an ice and water mixture circulated in the sample housing. The one completed cold temperature irradiation ($\sim 110^{o}K$) was performed using the irradiation cryostat described below. The damage was monitored during irradiation by periodically measuring the resistance of the sample at $78^{o}K$ which yielded a measure of the number of carriers removed.

C) Photoconductivity and Infrared Spectroscopy Measurements

Monochromatic light was supplied by a Perkin-Elmer model 98 monochromator capable of spanning the 1 to 10 micron wavelength range by using a variety of prisms.
Li F (1 to $\sim 6\mu$), CaF_2 (1 to $\sim 9\mu$), and NaCl (1 to $\sim 15\mu$). The monochromatic light was incident on the sample housed in a liquid nitrogen cryostat. The sample was cooled by immersion in helium gas kept at $78^{o}K$. In most of the photoconductivity spectra the light was

---

*We thank Dr. G. Brucker and Mr. D. Leibowitz of the RCA Laboratories for informing us of this technique

chopped at 13 cps and the signal generated by photoconductivity in the sample was fed to a Princeton Applied Research Corporation Model HR-8 lock-in phase sensitive amplifier with a PAR Model A preamplifier.

In order to achieve a high signal to noise ratio, the electronics and monochromator were enclosed in boxes made from ¼ inch thick aluminum plates. Furthers details can be found in reference 2.

It will be useful for examining the photoconductivity spectra to have a general idea of energy resolution. Naturally the energy resolution is kept as high as possible as allowed by the amount of signal available in any given sample. In all practical cases one choses a compromise energy resolution which allows a reasonable measure of signal within tolerable integration times. In Figure 1 we show the energy resolution plotted vs light energy for the Li F prism, while in Figure 2 we show energy resolution vs light energy for some typical runs made using the CaF_2 prism on sample JPL-36 before and after 15 minute anneals at each of the indicated temperatures. The discontinuous changes in the energy resolution curves shown in Figures 1 and 2 represent wavelengths where the entrance slit width is diminshed. The energy resolutions given in Figures 1 and 2 are typical of what we have utilized in our measured spectra and are intended to serve as a general guide when one examines the data from the PC spectra.

Wavelength calibration and energy resolution of the monochromator were obtained using a variety of gases and liquids which have well known absorption bands in the 1 to 15 micron wavelength range. The calibration sources we found most convenient were water $\sim 2.6\mu$, carbon dioxide $\sim 4.2\mu$, indene (C_9H_8) 2 to 8μ, polystyrene $(C_4H_2)_n(C_2H_3)_n$ 3 to 9μ and chloroform $CHCl_3$ 0.9 to 2.12μ.

The infrared spectroscopy measurements were made using either the Perkin-Elmer model 98 single beam single pass monochromator, or a Perkin-Elmer model 621 double beam infrared spectrophotometer. Additional details describing the infrared spectroscopy measurements may be found in another paper[4].

D) Irradiation Cryostat for Photoconductivity and Infrared Spectroscopy Measurements

The basic cryostat used in our work is an Andonian Associates liquid helium cryostat Model MHD-3L-30N equipped with a modified option 24 tail piece. The modified cryostat was used on previous work not associated with the task of the present contract. The details of the tail piece of the cryostat and how the light is admitted into the cryostat and allowed to pass through the sample has been described in detail elsewhere[6]. A combination of NaCl windows (at 300°K) and AgCl windows (78°K) are used to maintain the vacuum. Infrared light from 1 to 16 microns can pass through this window system. Temperature is controlled by means of heaters which vaporize the coolant liquid (N_2 or He) and either copper-constantan or gold (1% Fe) copper thermo-elements are used to sense the temperature.

The electron beam enters the cryostat at 90° with respect to the infrared light direction. Electrons first pass through a 0.0005" thick Kapton Polymide film* sealed with neoprene "O-rings" then through a cold

---

*Use of this film as a window material was suggested to us by Prof. John MacKay of Purdue University. The film is available from E. I. Dupont De Nemour & Co. (Inc.), Film Dept., Wilmington, Delaware 19898.

window 0.003" thick aluminum sealed with indium "O-rings" before striking the sample. The sample is mounted in such a way that it can be freely rotated in the sample holder through 360°.

III) Results

A) Irradiation of Lithium-Doped Si at ~300°K.

1) Photoconductivity Measurement

In all photoconductivity spectra measured at 78°K on samples irradiated at ~300°K we present the results in the form of plots relative photoconductivity $\frac{\Delta\sigma}{\sigma\Omega}$ (arbitrary scale) vs energy (eV) of the incident light. $\Delta\sigma$ represents the added conductivity due to the light incident on the sample of photon density Ω, and σ is the conductivity in the dark. The photoconductivity (PC) is plotted on a relative scale since the sample must be removed from the cryostat each time it is given an anneal in a separate high temperature (to ~ 650°C) oven. One cannot obtain an absolute measurement of PC since it is not possible to reproduce exactly the sample condition after it is taken out and re-inserted into the cryostat. However, in all cases we have normalized the spectra relative to the light source spectrum shape, thus permitting one to compare the shape of the measured photoconductivity spectra in a meaningful way. It is the shape of the spectrum which can yield energy level positions that are of importance in characterizing the defect. Of course the annealing effects on each level will be manifested by determining the relative PC associated with each energy level before and after a series of anneals.

In all annealing results we have performed isochronal annealing experiments with the sample kept at the annealing temperature for 15 minutes.

In Table I we have listed the characteristics of each sample for which results will be given in this report. The table lists the

lithium concentration, electron fluence and energy and the method of crystal growth. The starting material for all samples was 10 Ω-cm phosphorus doped $\sim$ 5 x 10^{14} phosphorus atoms/cm^3 and the sample orientation during irradiation was such that electrons were incident in the [III] direction (Note - since the samples were not oriented no other direction can be specified.

TABLE I - Lithium concentration, electron energy and fluence, and crystal growth method of samples studied in this investigation.

SAMPLE	JPL-17	JPL-11	JPL-69	JPL-12	JPL-36	*JPL-10
Li/cm^3	$2.0x10^{17}$	$9.0x10^{16}$	$9.0x10^{15}$	$7x10^{16}$	$5x10^{16}$	$5x10^{16}$
Fluence e/cm^2	$6.3x10^{17}$	$6.0x10^{17}$	$2.0x10^{17}$	$7.9x10^{17}$	$5x10^{17}$	$1.5x10^{17}$
Electron Energy	1.5 MeV	1.5 MeV	1.5 MeV	1.5 MeV	1.5 MeV	2 MeV
Crystal Growth	CG	CG	FZ	CG	CG	CG
Fluence/[Li(cm^{-3})]	3.2	6.7	22	11	10	3.0

*This sample was irradiated at $\sim$110°K.

CG - Crucible Grown FZ = Float Zone Refined

The resistance of each sample was found to increase by 2 to 4 orders of magnitude after irradiation and annealing in the temperature range 150 - 400°C. We have tabulated these rather striking increases* in resistance in Table II where we give the sample resistance measured at 78°K and at 300°K without light incident on the sample. Several of the samples resistances were measured with 1.3μ light shining on the sample. As can be seen in

* These increases in resistance are unique to Li-doped Si and we do not observe them in samples not containing lithium.

Table II, all samples exhibited pronounced increases in resistance which persisted up to annealing temperatures of 390°C and 450°C. We also observed this same effect on the sample irradiated at ~ 110°K in which dramatic increases in resistance were observed after anneals to 250°K. These results will be given below. The sample resistance before irradiation is also given in Table II, and as can be seen, large resistances are still found after anneals to 390 - 480°C. The large resistances would imply that the damage that remains is strongly compensating the donor impurities. We have not observed such effects in our previous [1] irradiations of Li-doped Si where infrared spectroscopy* was used to probe the defects. As an additional comment it is not reasonable to expect large changes in Li content to be brought about by 15 minute heat treatments of 350 - 400°C, when in fact, out-diffusion times on the order of one to several hours at ~ 450°C are utilized to cause re-distribution of lithium in our samples.

- - - - - - - - - - - - - - - - - -

* From the infrared absorption by free carriers.

TABLE II - Sample Resistance (in ohms) before and after irradiation and after 15 minutes annealing at each of the indicated temperatures. Resistance measured at 78°K and 300°K in the dark or with 1.3 μ light on the sample.

SAMPLE		Pre Anneal	150°C	200°C	300°C	340°C	390°C	480°C	Before Irradiation
JPL-69									
	300°K	6×10^{4} Ω	8×10^{5} Ω	6×10^{5} Ω	7×10^{4} Ω	2×10^{4} Ω			12 Ω
(in dark)	78°K	2×10^{7}	2×10^{10}	6×10^{11}	4×10^{10}	6×10^{10}	10^{12}		4
(with 1.3 μ)	78°K		2×10^{8}	3×10^{7}	2×10^{7}	2×10^{7}			
JPL-17									
	300°K	4	2×10^{4}	5×10^{4}	4×10^{4}	3×10^{6}			0.5
(in dark)	78°K	3×10^{7}	5×10^{10}	5×10^{10}	4×10^{12}	3×10^{11}	5×10^{11}	3×10^{11}	1.5
(with 1.3 μ)	78°K		1×10^{8}	2×10^{8}	4×10^{7}	10^{7}		3×10^{5}	
JPL-11									
	300°K	2	1×10^{5}	2×10^{4}	1×10^{4}	5×10^{5}	6×10^{5}		0.4
(in dark)	78°K	4×10^{7}	5×10^{11}	10^{11}	2×10^{11}	4×10^{8}	4×10^{11}	2×10^{4}	1.2
(with 1.3 μ)	78°K		6×10^{8}	1×10^{8}	3×10^{7}				
JPL-12									
	300°K	5	750						1
(in dark)	78°K	5×10^{6}	4×10^{11}	10^{12}					3
JPL-36									
	300°K	74	350	450					1.3
(in dark)	78°K	5×10^{7}	4×10^{11}	10^{12}					2.3

-16-

In Figure 3 we have shown the PC spectra for sample JPL-69 before anneal and after 15 minutes at 110, 300, 340, and 390°C. Although the sample was also given anneals at 150°C and 200°C no spectra could be measured as the impedance became too high (see Table II) and the voltage signal could not be accomodated by our equipment. For certain data points in the various spectra, we show the experimental uncertainty. These uncertainties represent the maximum values and for many of the points the error is less than the size of the plotted point. This same condition on uncertainty considerations and the presence of error bars for certain of the data applies on all subsequent results to be presented below. Note the evolution of peaks at energies of 0.82 and 0.99 eV after anneal at 300°C. After sample JPL #69 was annealed to 440°C, the signal to noise became very low indicating that little extrinsic photoconductivity remained and that the sample had nearly reverted to its pre-irradiation state. Another anneal to 480°C was made on this sample but no measurements were taken because of lack of time and program termination.

It is very important to realize the difficulty in assigning energy levels to specific "breaks" in the spectrum curve, i.e., the structure. In all results to be presented* we shall take as the energy level the point on the spectrum where the particular level exhibits the onset of ionization, and for all quoted energy levels the structure is such as to be outside the range of experimental error. In many cases it will be observed that the ionization of a "level" extends over a fairly broad energy and for some of the levels the width can be as large as $\sim$0.3 eV indicating that there are a large number of very closely spaced levels which cannot be resolved. We have observed this same phenomenon in radiation-produced

---

* Except for the peaks at 0.82, 0.99, 0.78 and 0.92 eV as shown in Fig. 3.

extrinsic PC for 1 to 100 Ω-cm phosphorus-doped Si which does not contain lithium.

In Figure 4 are shown the photoconductivity spectra for sample JPL -#17 before anneal and after 15 minutes at 100, 300, 340, 390, and 440°C. Here again no spectra could be measured after 150°C and 200°C anneals because of the high impedance problem mentioned above. After a 480°C anneal, no further signal could be measured on sample JPL-#17 due to a low signal to noise implying that the sample had nearly reverted to its pre-irradiation state. Note that the lithium content in sample JPL-#17 is approximately 20 times higher than for sample JPL-#69 (Figure 3). One feature of nearly all PC spectra is their wide range in the magnitude of PC ($\sim 10^5$) over the light energy range $\sim$ 0.2 to 1.0 eV. The spectra in Figure 4 do not exhibit the marked peaks in PC as were found at 0.82, and 0.99 eV, and at 0.78 and 0.92 eV, for sample JPL-#69. One can see some correlation of energy levels (Figures 3 and 4) which we shall discuss below.

Figure 5 shows the PC spectra for sample JPL-#11 before anneal and after 15 minutes at 100, 300, 340, 380, 420, and 450°C with spectra not shown after 150 and 200°C anneals for the same reason mentioned above. The spectrum measured after 450°C is very similar to what is obtained for unirradiated material containing lithium to a concentration of $\sim 5 \times 10^{16}$ cm^{-3}. In the results of Figure 5 we do not find peaks such as we observed in sample JPL-#69 (Figure 3). The lithium content for JPL-#11 (Figure 5) is $\sim$ 10 times larger than for JPL-#69 (Figure 3) where the peaks were observed. The extrinsic PC shown in Figure 5 appears to be controlled by 3 or 4 levels after each annealing treatment which also appears to be the case for the results shown in Figures 3 and 4.

Finally, in Figures 6 and 7 we present extrinsic PC for samples JPL-#12 and JPL-#36, respectively. Both samples were lithium doped to relatively high concentrations ($\gtrsim 5 \times 10^{16} cm^{-3}$). No further spectra were measured on these samples for anneals to temperatures above 200°C due to lack of time. Both of the samples (shown in Figures 6 and 7) exhibit extrinsic PC which appears to be controlled by 3 or at most 4 energy levels, and in both cases we see marked effects on the spectrum which was measured after 200°C anneal.

2) Infrared Spectroscopy Measurements

All samples irradiated at $\sim$ 300°K were given fluences of 1.5 MeV electrons which were either less than or equal to $\approx 7.9 \times 10^{17} e/cm^2$. We did not observe any radiation-induced infrared active absorption bands. This result is in agreement with and consistent with our previous studies[7] which showed that $\sim$ 5 MeV electron fluences of $< 10^{18} e/cm^2$ do not induce sufficient numbers of infrared active centers. In one particular experiment we made a detailed search for radiation defect bands in a high purity (20,000 Ω -cm) float-zone refined Si sample lithium diffused to 4×10^{16} Li atoms/cm^3 (0.18 Ω -cm). The sample was irradiated at $\approx$ 295°K with 5 MeV electrons to a fluence of $3.3 \times 10^{17} e/cm^2$. No radiation-induced infrared-active bands were found in the wavelength range $\approx$1 to 50 μ. Infrared spectrum measurements were made with the sample at 300°K and at 78°K.

B) Irradiation of Lithium-doped Si at $\sim$ 110°K.

1) Photoconductivity Measurements

The resistance of one lithium-doped Si sample irradiated at 110°K exhibited a very rapid increase in resistance at 78°K after the cessation of

the irradiation. In addition, this sample also underwent rapid changes in resistance before and after anneals to 250°K. We have summarized these results pictorially in Figure 8 where we plot sample resistance (measured at 78°K) vs time after the irradiation was stopped. We can immediately see that since nearly all the free carriers were removed in the irradiation the resistance is extremely sensitive to some defect which may undergo an intermediate step whereby a complex defect having increased carrier trapping power may be formed. This is only conjecture, the process causing the behavior is not understood. During the time the PC spectrum was measured after each anneal the sample impedance remained stable. The time needed to measure the spectrum was approximately 60 minutes. The photoconductivity spectra results are given in Figure 9 for sample JPL-#10. Note that JPL-#10 was irradiated to a 2 MeV electron fluence of $1.5 \times 10^{17} e/cm^2$, and that the sample temperature during bombardment was kept below 110°K.

Since the sample was not taken out of the cryostat during the entire experiment it is possible to compare the relative photoconductivity after each anneal. It should be pointed out that the spectra in Figure 9 have not been normalized for the light source and appear to have markedly different spectrum shape above $\sim$ 0.6 eV than other light source normalized spectra; Figures 3 - 7. The important results to be extracted from Figure 9 are the apparent recovery of the peak at 0.34 eV around 250°K, and the presence of a dominant level at E_c-0.4 eV. The result clearly illustrates that annealing or re-orientation of the defect responsible for the PC peak at E_c-0.34 eV is occuring in the 200 to 250°K range. This implies that for Li concentrations of $\sim 5 \times 10^{16} cm^{-3}$ exposed to fluences of $10^{17} e/cm^2$

motion of defects occurs which has large effects on the sample properties, and although Li is not diffusing in the Si lattice matrix at these temperatures, other primary defects, vacancies and interstitials, must be sufficiently mobile so as to alter the defect structure.

The results on the cold temperature irradiation also show that the radiation-induced extrinsic photoconductivity (PC) is controlled by 3 or 4 dominant defect levels. The infrared spectra were measured for sample JPL #10 (Figure 9) after each anneal and no defect infrared active absorption bands were found. It is of some relevance to compare Si doped with Li with silicon doped with P and As to $\sim$ 5 - 10 x 10^{16} atoms/cm^3 in which all the materials are bombarded by $\lesssim$ 2 MeV electrons to fluences of $\sim$ 2 - 5 x 10^{17} e/cm^2. In the case of P- and As-doped Si we have observed[8] infrared active bands in the $\approx$ 8 to 10 micron wavelength region, which we attribute to defect complexes consisting of at least two impurity atoms (P or As) and a single vacancy as constituents making up the infrared active center. The observed spectra are found to arise from electronic transitions and detailed piezospectroscopic studies have shown the center exhibits a monoclinic II symmetry with orientational degeneracy. Thus far we have not found bands of this kind in Li-doped Si.

IV) DISCUSSION OF RESULTS

It is very difficult to characterize all the imperfections present in the crystal before irradiation. This fact adds to the additional complexity which arises from radiation produced(or assisted) imperfections. The presence of oxygen has been well established although no simple method yet exists to accurately pinpoint the oxygen concentrations which includes oxygen atom configurations which are not infrared active. Moreover, when the oxygen concentration is lower than $\sim 1 - 5 \times 10^{16}$ cm^{-3} it is not possible to use IR spectroscopy* to measure the oxygen content below 5×10^{15} cm^{-3} due to the weak intensity of the 9μ band characteristic of vibrational modes of interstitial oxygen in Si. More recently the presence of carbon[9,10,11] in Si has been found to produce complexes which arise from the vibration of carbon atoms coupled to a radiation-induced defect, more probably vacancies and/or divacancies. In some recent radiation-induced extrinsic PC studies in Si by Young,[12] it was found that a level near E_C - 0.4eV is always present before irradiation of P-doped Si. The early electron paramagnetic resonance studies[13] on the phosphorus-vacancy pair (E-center) with its associated level at E_C - 0.40 eV may be present before irradiation and could be due to vacancy-phosphorus complex pairs which are formed in the diffusion process during growth of the crystal. Finally, there are present in the material crystal imperfections such as dislocations detectable as etch pits or by X-ray techniques.

- - - - - - - - -- - - - - - -

* For the latest development on infrared spectroscopy measurements of oxygen in Si see J. A. Baker, Solid State Communications, Vol. 3, 143 November 1970.

Now, on top of all the above mentioned imperfections we introduce further complexities in our system due to the presence of radiation damage (vacancies, divacancies, interstitials, etc.), and lithium atoms whose concentration we infer from their electrical activity (as deduced from conductivity measurements). The concentrations of lithium quoted in Table I may all be too low (perhaps by a factor $\sim$ 3 to 5) since we do not measure lithium which has clustered into aggregate forms, and hence, been rendered electrically inactive. Based on our past experience, we do not expect that the electrically inactive lithium plays an important role in the radiation damage process, particularly as monitored by extrinsic PC and infrared spectroscopy. However, it may be possible that as lithium atoms dissociate they become electrically active, we have no proof of this.

In comparing and correlating our results with other workers who have studied radiation damage in Li doped Si using $\lesssim$ 5 MeV electrons it is not a simple and straight forward matter to compare the energy levels we have observed in our photoconductivity measurements with those obtained by carrier concentration, photoluminescence and minority carrier lifetime temperature dependence. This is because of the fact that the different measurements may not all be looking at the same defects in the same charge state. For example Brucker[14] finds a level at E_c-0.12eV (and in some cases deeper levels not amenable to study by carrier concentration) in oxygen-lean low Li-containing Si. Brucker determined that the level anneals out at 373°K after bombardment of the sample at 80°K to $\sim$ 200°K. Additionally, Brucker[15] has also found shallow levels in cold temperature irradiation of Si, one at E_c-0.08eV (requires Li), and the other at E_c-0.13eV (not depending on presence of Li). We have not detected such shallow levels in our work

but this may be due to our different experimental conditions, i.e., our higher irradiation temperature ($\sim$ 300°K) and higher Li concentration 10 to 100 times higher than the lithium content in Brucker's[14,15] samples. Our low energy measuring capability extended to 0.11eV, in the figures our spectra cutoff at an energy below which we lose PC signal.

A level at E_c-0.4eV (or greater) in oxygen-lean P-doped Si has been reported by Carter[16] who has "tentatively attributed" this level to a Li-vacancy pair. In view of the fact that we observe such a level in many of our oxygen-containing samples and also in non-lithium containing[5] Si, the interpretation of Carter may not be correct. We have given strong evidence[6] that the level near E_c-0.4eV (from PC) is associated with the divacancy defect in its -2 charge state. Moreover, the measurement of Carter (carrier concentration) cannot pinpoint the position accurately because of the limitation of carrier concentration measurements when one has to locate deep levels $>$ 0.35eV from the conduction band edge.

It is interesting to note that both Naber[17] and Curtis[18] report a level near E_c-0.4eV in lightly Li-doped Si ($\sim 5 \times 10^{14}$ Li/cm^3) which participates in the recombination process. This recombination level may be associated with the divacancy or a complex requiring a Li atom as suggested by Curtis[18].

It is worthwhile to make one further comparison of our results with the work of W. Dale Compton[19] who has used photoluminescence to determine energy level positions in 3 MeV electron irradiation of Li-diffused Si. In summary, Compton[19] has found levels in both lithium-free and lithium-containing irradiated Si. We shall only be interested in comparing our

results with Compton's work on Li-containing Si. Compton quotes his energy levels relative to a band edge and has found[20] a level at 1.045eV in both oxygen rich (CG) and oxygen-lean (FZ) Si after a 3 MeV electron irradiation to $10^{18}e/cm^2$. The 1.045eV level anneals out between 350 - 400°C in CG Si and between 400 - 450°C in FZ Si and does not occur without the presence of Li. Compton finds three other dominant levels at 0.78, 0.87, and 1.00eV which can be observed only if both oxygen and lithium are present in the sample, these levels are not observed in FZ Si doped with Li. The annealing properties of these levels are summarized below. . .

. . .the 1.00eV level first appears after 400°C anneal then anneals out after 600°C heat treatment;

. . .the 0.78eV level first appears after 200°C anneal with subsequent disappearance after 400°C anneal;

. . .the 0.87eV in P-type appears at 200°C and anneals out at 300°C, while in n-type the level anneals out at 300°C.

One very important characteristic of the photoluminescence measurements is that one must irradiate the sample to relatively high fluence ($\sim 10^{18}e/cm^2$) in order to observe levels. The fluences necessary to observe damage in PC were a factor 2 to 10 smaller and this may have the effect of causing somewhat different defect configurations to be observed. The difference in fluence becomes even more pronounced when photoluminescence is compared to carrier concentration and lifetime measurements where the fluences used are in the much lower range 10^{14} - $10^{17}e/cm^2$.

We have summarized all the radiation-produced levels observed from PC in our samples in Figure 10. We also show the levels observed in electron-irradiated (1.5MeV) P-doped Si, both CG and FZ, which were not doped with Li. (Samples Rosa I and II). These Li-free samples are useful in that they give us some information on the background radiation-induced extrinsic PC. In noting the levels given on Figure 10 it is very important to realize that after any given anneal, only 3 or 4 levels dominate the PC for any particular sample (see Figures 3 - 7 and Figure 9), whereas we included in Figure 10 all observed levels. Evidently, then, these results imply that after heat treatment defects are re-orienting and perhaps recombining in such a way that the energy levels shift. Our PC measurements have shown that there are more localized defect energy levels in the forbidden gap than have been reported in photoluminescence, carrier concentration, and lifetime measurements which we believe arises from our combined greater energy resolution and sensitivity than the other just mentioned measurement probes. Clearly the photoluminscence has the advantage of greater energy resolution than PC, but has lower sensitivity to defect levels than PC.

It is difficult to correlate our energy levels with those obtained by Brucker[14] since we may be looking at different specific defects due to the fact that he[14] finds much lower recovery temperatures (300 - 373°K) than those we obtain in our case (in the range 400 - 700°K). However, the lithium associated recombination level reported by Curtis[18] at E_c-0.4eV may also be one of the levels we measure in the range E_c-0.35 to E_c-0.42eV, (see Figures 3, 4, 5, 6, 7 and 9). The annealing temperature determined by Curtis

of 253°C does not correlate well with our heat treatment recovery temperatures. Carter[16] using carrier concentration also finds deep levels at E_C-0.4eV or deeper in electron-irradiated Li-diffused Si. However, in reference 16 Carter does not report on the annealing properties of the level (or levels), although the energy level position correlates with our findings from PC.

It is most likely that our results can be correlated best with Compton's[19,20] photoluminescence studies since the levels observed by Compton appear to be affected by heat treatment in the same temperature range 200 - 600°C as in our case. Moreover considering the uncertainty as to which band edge the levels refer to, we can surmise that the photoluminescence levels at 1.00, 0.87, and 0.78eV in CG Si can also be counted among those found in our samples (see Figure 10).

In view of the complexities of the radiation damage problem and the added complication that many of the radiation-produced energy levels lie deep in the forbidden gap, it is not possible to make significant theoretical analysis of the results. The main reason for the difficulty in the analysis is that little or no information is available on wave functions for electrons in deep lying states. Some success has been obtained using effective mass theory for shallow donors and Fan[21] has calculated the photoexcitation cross section based on a 1S ground state for electron excitation in hydrogen. For the case $h\nu \gg \Delta E$, where $h\nu$ is the incident energy and ΔE the energy below the conduction band (binding energy of the electron in the defect) the photoexcitation cross section calculated by Fan[21] is

$$\sigma \sim 8.5 \times 10^{-15} \left(\frac{\Delta E}{h\nu}\right)^{7/2} cm^2$$

If our energy levels are used then the calculated cross sections tend to have magnitudes of $\sim 10^{-16} - 10^{-17}cm^2$, and the calculated energy dependence in σ is roughly comparable to what is measured.

Recently some theoretical work has been reported by Bebb[22] who used the quantum defect method to calculate optical absorption processes for deep lying chemical impurity states in semiconductors. Although not directly applicable to our case we attempted to analyze our results for deep lying radiation-produced "impurity states" using Bebb's theory. No other theory is presently available and although not germane to our case it was our intention to apply it as a first approximation. Bebb obtains approximate wave functions to describe deep lying impurity states. However, a main conclusion of Bebb appears to be in disagreement with what we measure, namely the PC which is proportional to the photoexcitation cross section is always found to decrease with decreasing defect energy (from the conduction band) whereas Bebb's theory predicts just the opposite. One other limitation of the Bebb theory is that it predicts the same cross section for all impurities having the same localized energy state in the forbidden gap. This theoretical conclusion seems to be an oversimplification for the case of radiation defects which may have different complex configurations in which the probability for promoting an electron to the conduction band by photoexcitation may be different for each defect even though the energy levels may be very close to the same position in the forbidden gap as in the case of E - center, $\approx E_C - 0.40eV$, and divacancy, $\approx E_C - 0.39eV$. We conclude that the theory in its present simplistic form cannot be used fruitfully to

to interpret the data, while recognizing the formidable complexity of the problem other approaches may be necessary, we wish to briefly describe one approach here.

If detailed measurements of defect introduction rate were made, and if one were able to make positive identification of the defect with an energy level, then one could compare the theoretical cross section with measured values and make improvements in the model and theory to accurately fit the data. Although this is a phenomonological approach at this time, we can propose no simple alternative.

V) CONCLUSIONS

Electron irradiation ($\lesssim$ 2 MeV) of oxygen-lean and oxygen-rich Si doped with Li from 9 x 10^{15}Li/cm^3 to 2 x 10^{17}Li/cm^3 produces lithium-associated defect complexes which give rise to localized energy levels in the forbidden gap. Levels giving rise to extrinsic PC are formed at $\approx$ E_c-0.2, E_c-0.4, E_c-0.54, and E_c-0.6, E_c0.7, and E_c-0.8 eV in CG material, while in FZ material the dominant levels are at $\approx$ E_c-0.2, E_c-0.54, E_c-0.65, E_c-0.8, E_c-0.92, and E_c-1.0 eV. Heat treatment to temperatures in the range 100 - 450°C produces pronounced disappearance (recovery) of some levels and appearance of new (or shifted) energy levels. Wherever possible, we have been able to correlate our measured energy levels with those obtained from carrier concentration, minority carrier lifetime and photoluminescence, in particular, the level at E_c-0.4eV.

Our measured annealing temperature ranges are consistent with those obtained in irradiated Li-doped solar cells by Fang and Iles[23] who report annealing stages at 100 - 150°C and at 300 - 450°C. Additionally photoluminescence also yields annealing temperatures roughly consistent with our values (200 - 450°C).

The PC spectrum obtained in samples containing lithium to concentrations $\gtrsim$ 5 x 10^{15}cm^{-3} in general contains more structure indicative of greater complexity than the spectrum measured in the same starting silicon material not containing lithium.

No infrared active defect absorption bands are observed (1 to 50 microns) in samples irradiated by electrons ($\lesssim$ 5 MeV) to fluences of 3.3 x 10^{17}e/cm^2.

One cold temperature irradiation experiment run at 110°K shows that annealing or re-orientation of Li-associated defects occurs at temperatures between 200 - 250°K. In all cases we observed large increases in resistivity with continued heat treatment in the temperature range 150°K up to 700°K.

No satisfactory theoretical analysis of the data can be made using any of the presently published theories.

ACKNOWLEDGMENT

Most of the measurements were made by Mr. Thomas Mortka and Mr. Edward Fenimore and their careful conduct of the experiments is gratefully acknowledged. We also acknowledge the careful reading of the manuscript of this report by Dr. R. Stirn of JPL who made constructive criticisms to improve the report.

APPENDIX

Areas of Research Recommended for Future Work

On the basis of our past program we find that there are two areas where further study and improvement of measurement techniques would greatly add to an understanding of the radiation damage process. The areas are described below.

1.) The measurement of PC curve can be made with greater accuracy in the determination of the energy level position if one employed modulation spectroscopy. In this method one is able to extract the critical structure of energy levels in the spectrum which is usually superimposed on a large uniform background, thereby obtaining a more detailed picture of "line shapes". The modulation spectroscopy method involves oscillation of one of the mirrors present in the light beam path after the monochromator. This yields a modulation of amplitude of PC signal and wavelength and what one then measures is the derivative of PC, i.e., $\frac{d}{d\lambda}\left(\frac{\Delta\sigma}{\sigma\Omega}\right)$. In this modulation measurement one should, in principle, be able to obtain energy peaks, where without modulation one obtains just $\frac{\Delta\sigma}{\sigma\Omega}$. Details of this technique may be found elsewhere* and further analysis is needed to show how this modulation method would apply+.

2.) In order to determine whether the PC arises from holes or electrons which would answer the question as to whether a particular PC energy level arises from the excitation of an electron to the conduction band, or from excitation of a hole to the valence band, one would use a magnetic field to

---

* K. L. Shaklee, J. E. Rowe, and Mr. Cardona, Phys. Rev. 174, 828 (1968)

K. L. Shaklee, Ph.D. Thesis, Brown University, 1968 (unpublished)

+ W. G. Spitzer, Univ. of Southern Calif. has applied this method to IR absorptions, we feel "intuitively" it should work for PC.

distinguish between electrons and holes in a sort of photo-Hall measurement. Construction of this system with new optics would require a considerable effort ($\sim$ 2 man months).

Successful implementation of both items (1) and (2) above would require a fairly concentrated effort which was not included in the primary goal of the present program. We strongly recommend that some researcher be given the opportunity to work on the above ideas in order to improve experimental results assisting in characterizing the radiation-induced extrinsic PC.

REFERENCES

(1) R. C. Young, J. W. Westhead and J. C. Corelli. J. Appl. Phys. 40, 271 (1969)

(2) J. C. Corelli and T. Mortka, "Investigation of the Structure of Radiation Damage in Li-Diffused Si". Final Report 3 February - 8 December 1969. JPL Contract No. 952456

(3) J. C. Corelli, "Investigation of the Structure of Radiation Damage in Lithium Diffused Si". Midway Report. 1 January - 1 June 1970 JPL Contract No. 952456

(4) L. J. Cheng, J. C. Corelli, J. W. Corbett and G. D. Watkins. Phys. Rev. 152, 761 (1966)

(5) R. C. Young and J. C. Corelli, Progress Reports to Air Force Cambridge Research Laboratories, April 1970, September 1970, (unpublished), Rensselaer Polytechnic Institute, Troy, New York

(6) A. H. Kalma and J. C. Corelli. Phys. Rev. 173, 734 (1968)

(7) R. C. Young, unpublished data, Rensselaer Polytechnic Institute, (1969)

(8) C. S. Chen, J. C. Corelli, G. D. Watkins, Bull. Am. Phys. Soc. 14, 395 (1969)

(9) F. L. Vook, and H. J. Stein, Appl. Phys. Lett. 13, 343 (1968)

(10) A. R. Bean and R. C. Newman, Solid State Comm. 8, 175 (1970)

(11) A. Brelot and J. Charlemagne, "1970 Int'l Conf. on Radiation Effects in Semiconductors", State Univ. of N. Y. at Albany, 24-26 August 1970, to be published in "Radiation Effects" 1971.

(12) R. C. Young, unpublished data, Rensselaer Polytechnic Institute 1970

(13) G. D. Watkins, J. W. Corbett, Phys. Rev. 134, A1359 (1964)

(14) G. Brucker, Third Quarterly Report, RCA Contract with JPL #95255 1 January - 31 March 1970

(15) G. Brucker, Phys. Rev. 183, 712 (1969)

(16) J. Carter - TRW Systems Group, Progress Report No. 13154-6011-R0-00 to JPL on Contract #952554 (19 June 1970)

(17) J. Naber, Gulf General Atomic, Progress Report No. GA-9909 (23 January 1970) to JPL on Contract #952387.

(18) R. F. Bass, O. L. Curtis, Jr., and J. R. Srour, Northrop Corporate Laboratories, Final Progress Report No. NCL-51R to JPL on Contract #952523, August,1970.

(19) W. Dale Compton, Progress Report, 15 July 1970 to JPL on Contract #952383, University of Illinois.

(20) E. S. Johnson and W. D. Compton, "1970 International Conference on Radiation Effects in Semiconductors". State University of New York at Albany, 24-26 August, 1970 (to be published).

(21) H. Y. Fan, Repts. Prog. Phys. XIX, 107 (1956)

(22) H. B. Beeb, Phys. Rev. 185, 1116 (1969)

(23) P. H. Fang, and P. Iles, App. Phys. Letters, 14, 131 (1969)

FIGURE CAPTIONS

Figure 1) Typical energy resolution curve used in photoconductivity measurements made with a LiF prism. The energy resolution Δ E (eV) is plotted vs energy (eV) and the corresponding wavelength (μ).

Figure 2) Typical energy resolution curves used in photoconductivity measurements made with a CaF_2 prism. The energy resolution Δ E (eV) is plotted vs energy (eV) for sample JPL #36 after various 15 minute anneals at the temperature shown.

Figure 3) Relative photoconductivity $\frac{\Delta\sigma}{\sigma\Omega}$ vs energy of light for sample JPL #69 after irradiation (at $\approx$ 300°K) and annealing (15 minutes at each temperature). Also shown is the spectrum for unirradiated material. Energy level positions (eV) are shown by vertical arrows and error bars for measurements with largest experimental uncertainty, and similarly in Figs. 4-7.

Figure 4) Relative photoconductivity $\frac{\Delta\sigma}{\sigma\Omega}$ vs energy of light for sample JPL-#17 after irradiation (at $\approx$ 300°K) and annealing (15 minutes at each temperature).

Figure 5) Relative photoconductivity $\frac{\Delta\sigma}{\sigma\Omega}$ vs energy of light for sample JPL #11 after irradiation (at $\approx$ 300°K) and annealing (15 minutes at each temperature). The spectrum before irradiation closely resembles the one marked 450°C.

Figure 6) Relative photoconductivity $\frac{\Delta\sigma}{\sigma\Omega}$ vs energy of light for sample JPL-#12 after irradiation (at $\approx$ 300°K) and annealing (15 minutes at each temperature).

Figure 7) Relative photoconductivity $\frac{\Delta\sigma}{\sigma\Omega}$ vs energy of light for sample JPL-#36 after irradiation (at $\approx$ 300°K) and annealing (15 minutes at each temperature).

Figure 8) Dependence of resistance for sample JPL-#10 on time after irradiation (at $\approx$ 110°K) and anneal for 15 minutes at the temperatures shown.

Figure 9) Relative photoconductivity $\frac{\Delta\sigma}{\sigma}$ vs energy of light for sample JPL-#10 after irradiation (at $\approx$ 110°K) and annealing (15 minutes at each temperature).

Figure 10) Composite of all the radiation-induced energy levels found from photoconductivity in Li-doped samples studied in this investigation (see Tables I and II). For comparison we also show levels found in FZ and CG 10 Ω-cm P-doped Si which was the starting material that was Li-diffused in these studies.

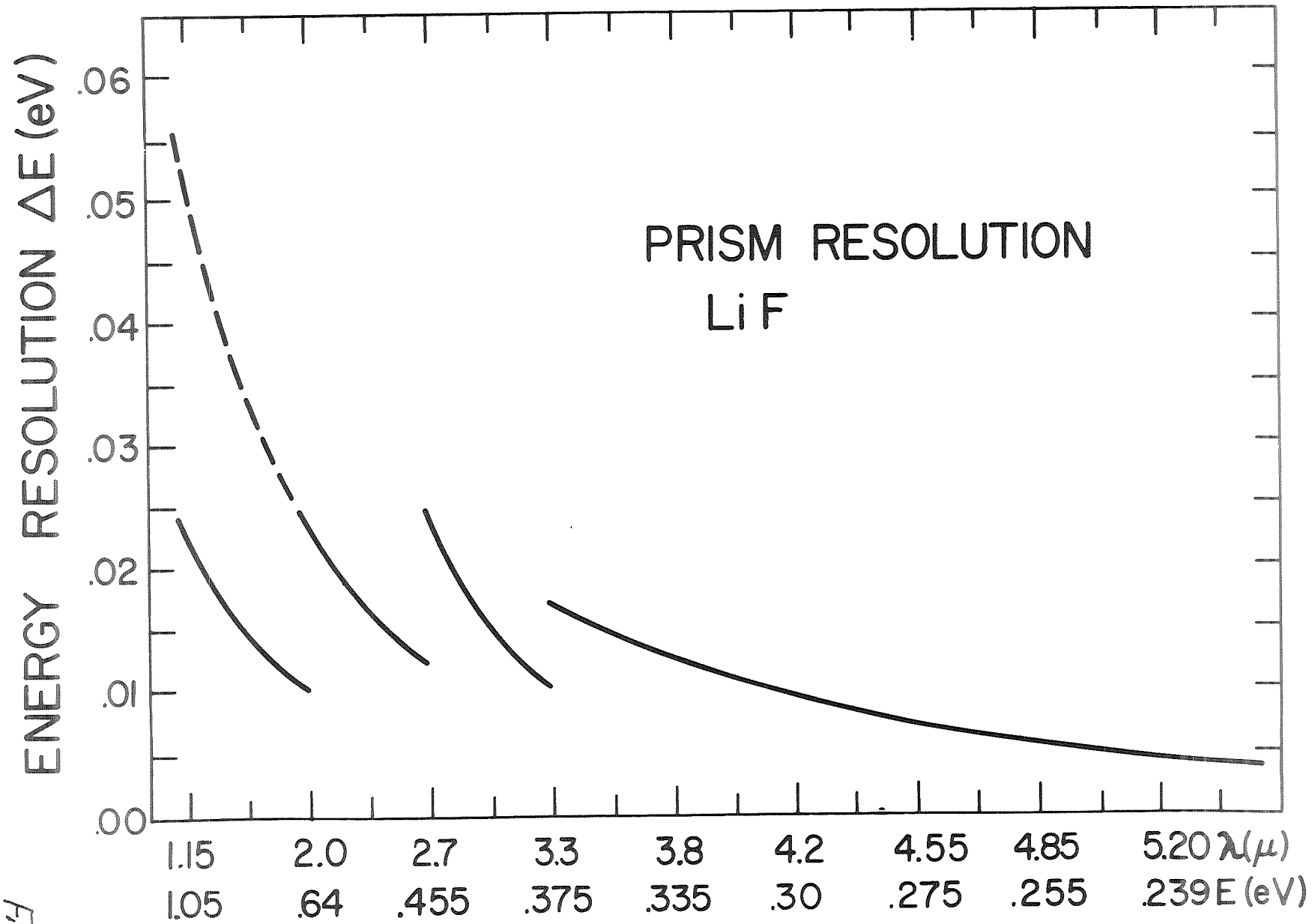
PRISM RESOLUTION
LiF
ENERGY RESOLUTION ΔE (eV)
.06
.05
.04
.03
.02
.01
.00
1.15 2.0 2.7 3.3 3.8 4.2 4.55 4.85 5.20 λ(μ)
1.05 .64 .455 .375 .335 .30 .275 .255 .239 E (eV)

Fig. 1)

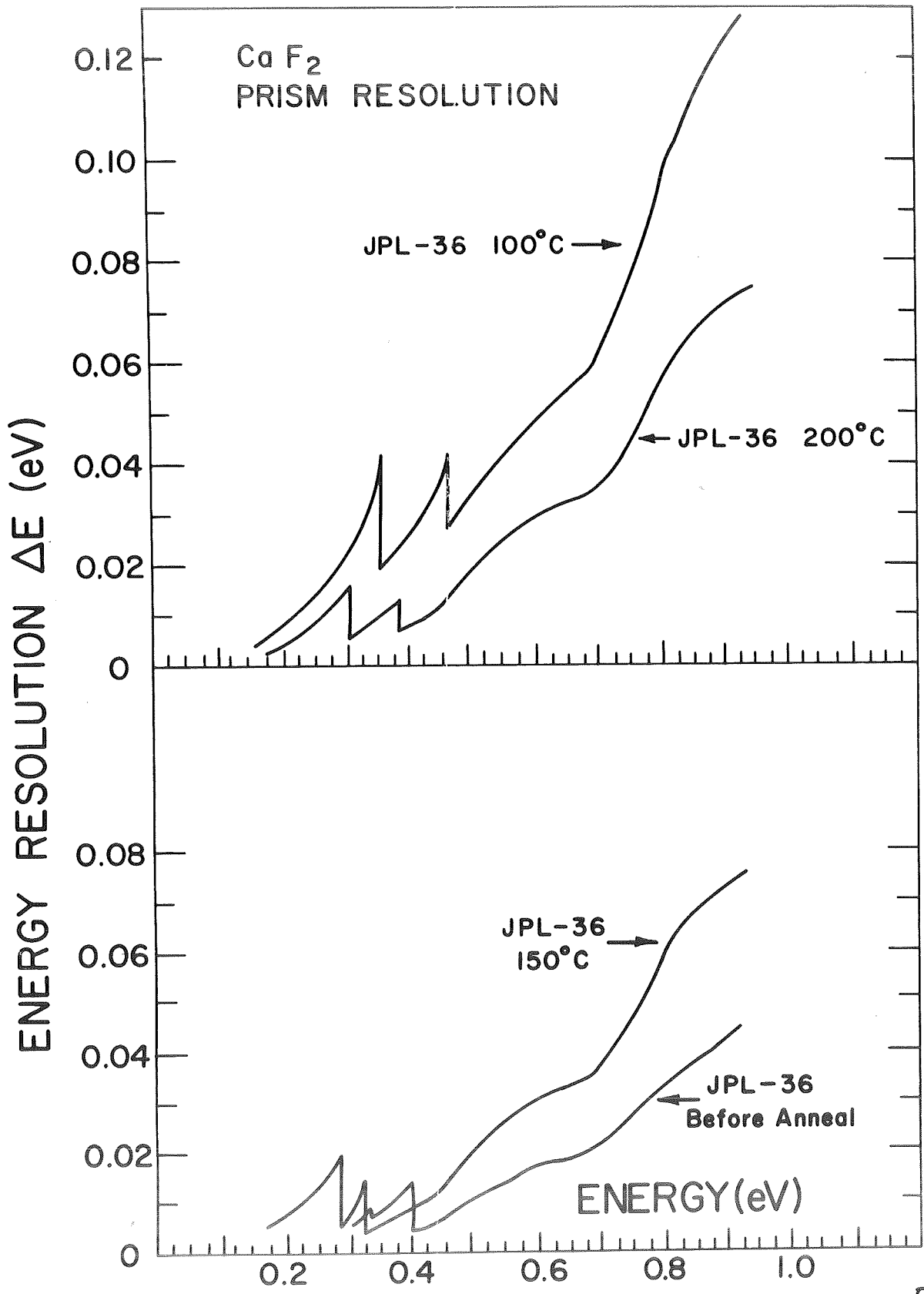
Ca F2
PRISM RESOLUTION
JPL-36 100°C
JPL-36 200°C
JPL-36
150°C
JPL-36
Before Anneal
ENERGY RESOLUTION ΔE (eV)
ENERGY(eV)
0.12
0.10
0.08
0.06
0.04
0.02
0
0.2
0.4
0.6
0.8
1.0

Fig. 2.)

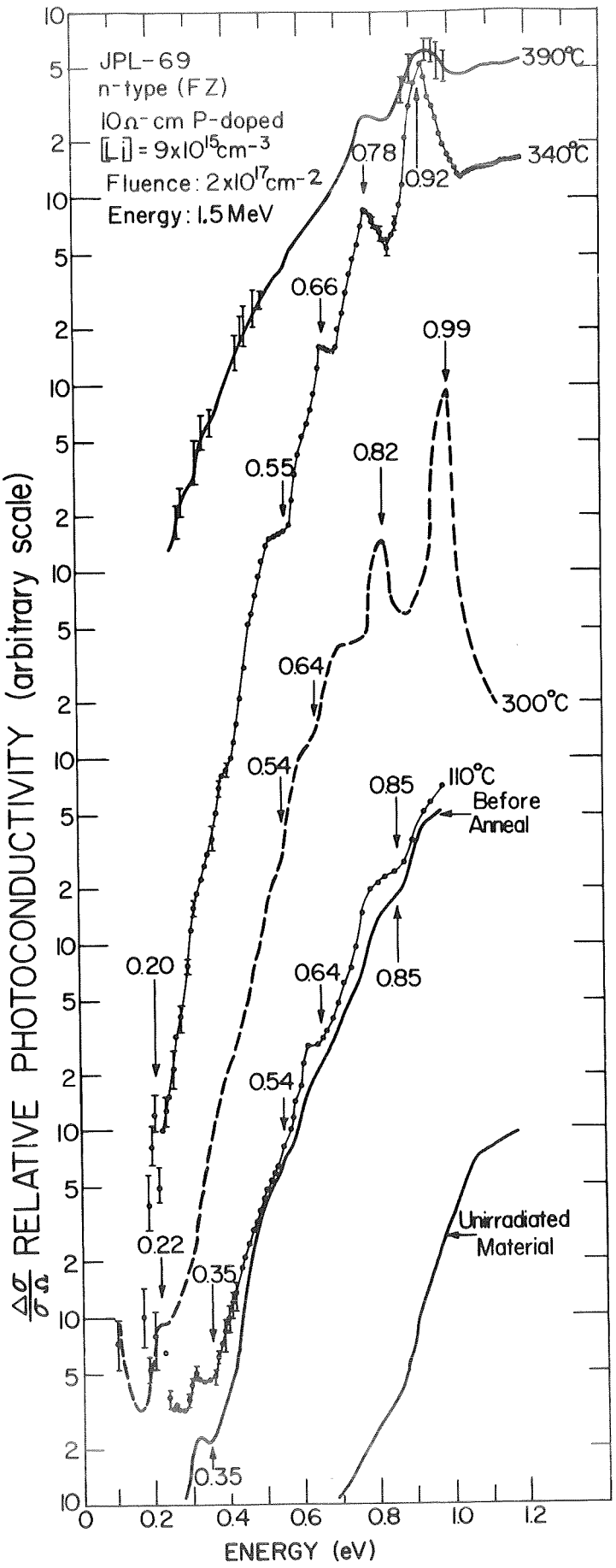
JPL-69
n-type (FZ)
10Ω-cm P-doped
[Li] = 9x10^15 cm^-3
Fluence: 2x10^17 cm^-2
Energy: 1.5 MeV
390°C
340°C
300°C
110°C
Before
Anneal
Unirradiated
Material
0.78
0.92
0.66
0.99
0.55
0.82
0.64
0.54
0.85
0.20
0.64
0.85
0.54
0.22
0.35
0.35
Δσ/σΩ RELATIVE PHOTOCONDUCTIVITY (arbitrary scale)
ENERGY (eV)
0
0.2
0.4
0.6
0.8
1.0
1.2

Fig. 3.)

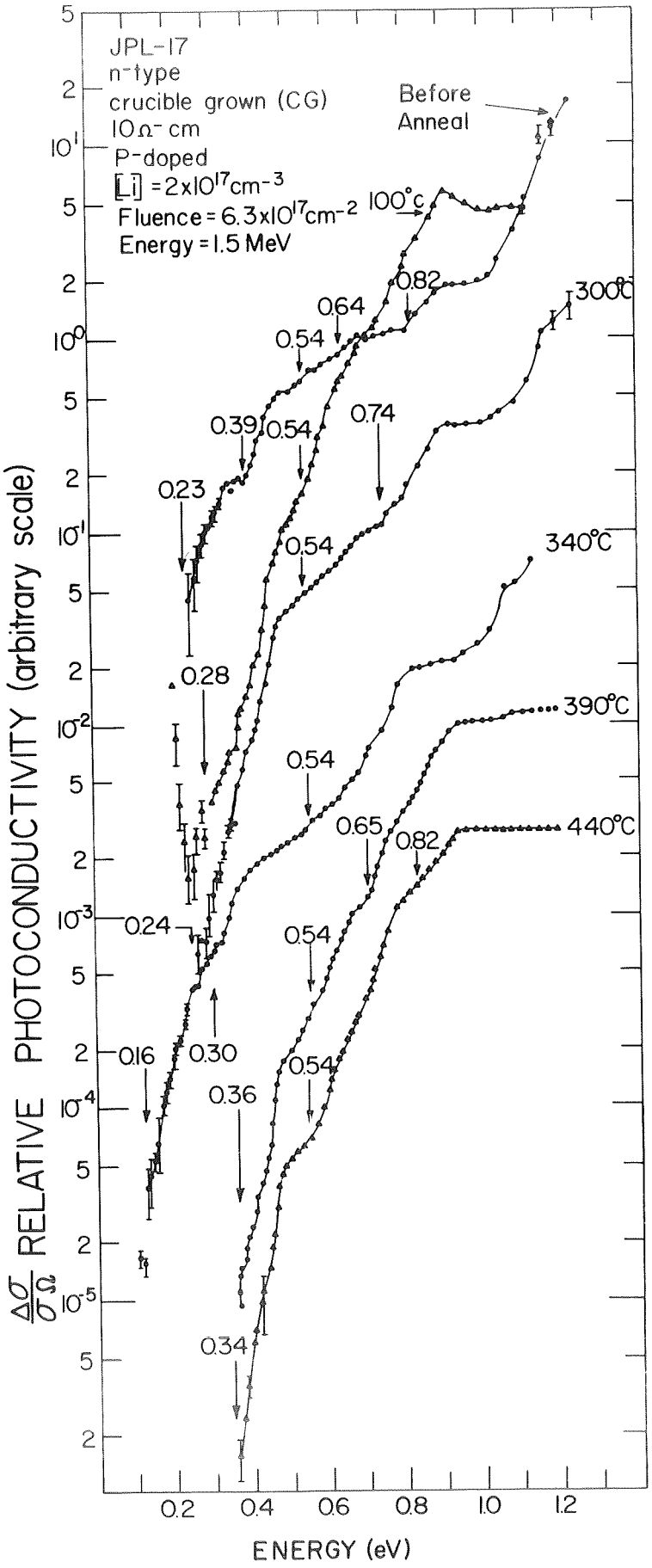
JPL-17
n-type
crucible grown (CG)
10Ω-cm
P-doped
[Li] = 2x10^17 cm^-3
Fluence = 6.3x10^17 cm^-2
Energy = 1.5 MeV
Before Anneal
100°C
300°C
340°C
390°C
440°C
0.82
0.64
0.54
0.39
0.54
0.74
0.23
0.54
0.28
0.54
0.65
0.82
0.24
0.54
0.16
0.30
0.54
0.36
0.34
ΔσRELATIVE PHOTOCONDUCTIVITY (arbitrary scale)
ENERGY (eV)
0.2
0.4
0.6
0.8
1.0
1.2

Fig. 4.)

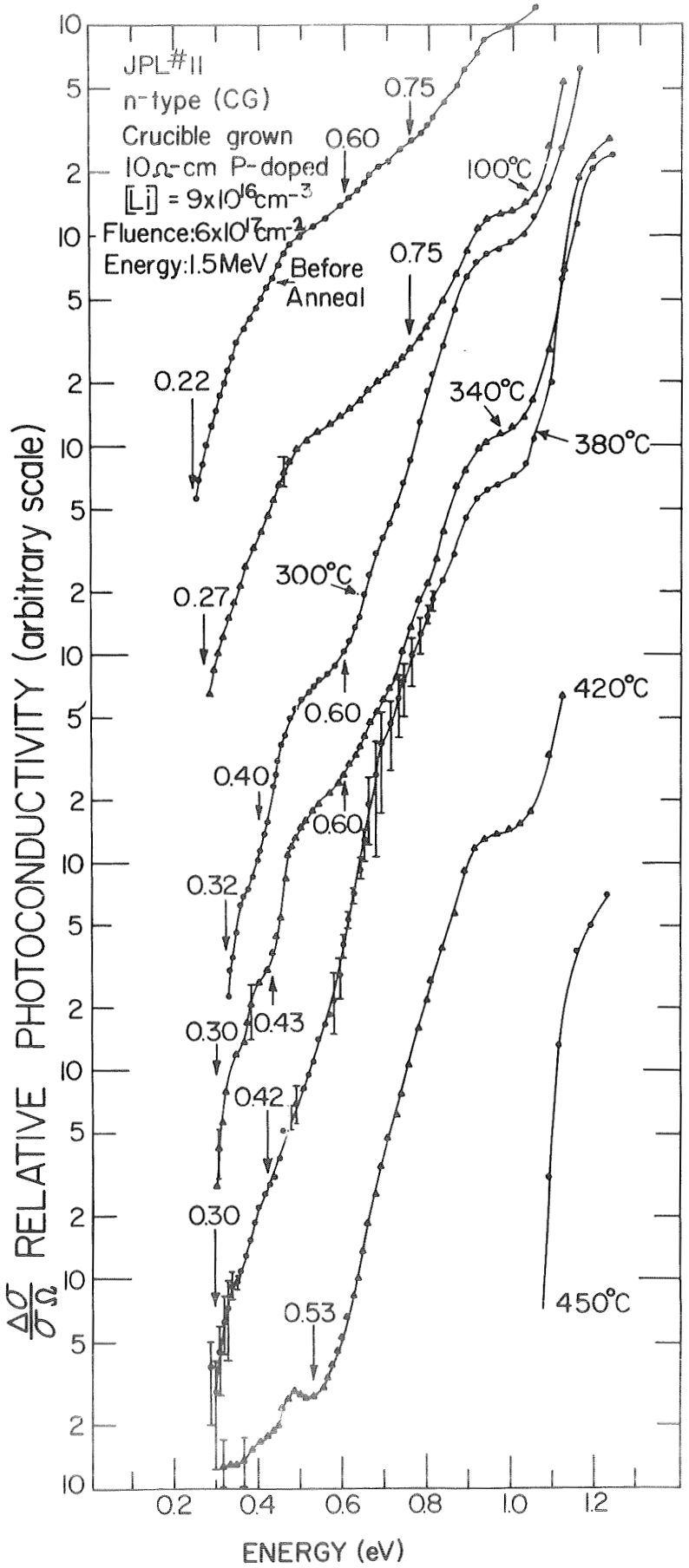
JPL#11
n-type (CG)
Crucible grown
10Ω-cm P-doped
[Li] = 9x10^16 cm^-3
Fluence: 6x10^17 cm^-2
Energy: 1.5MeV
Before Anneal
0.75
0.60
100°C
0.75
0.22
340°C
380°C
300°C
0.27
0.60
420°C
0.40
0.60
0.32
0.43
0.30
0.42
0.30
0.53
450°C
Δσ/σΩ RELATIVE PHOTOCONDUCTIVITY (arbitrary scale)
ENERGY (eV)
10
5
2
0.2
0.4
0.6
0.8
1.0
1.2

Fig. 5.)

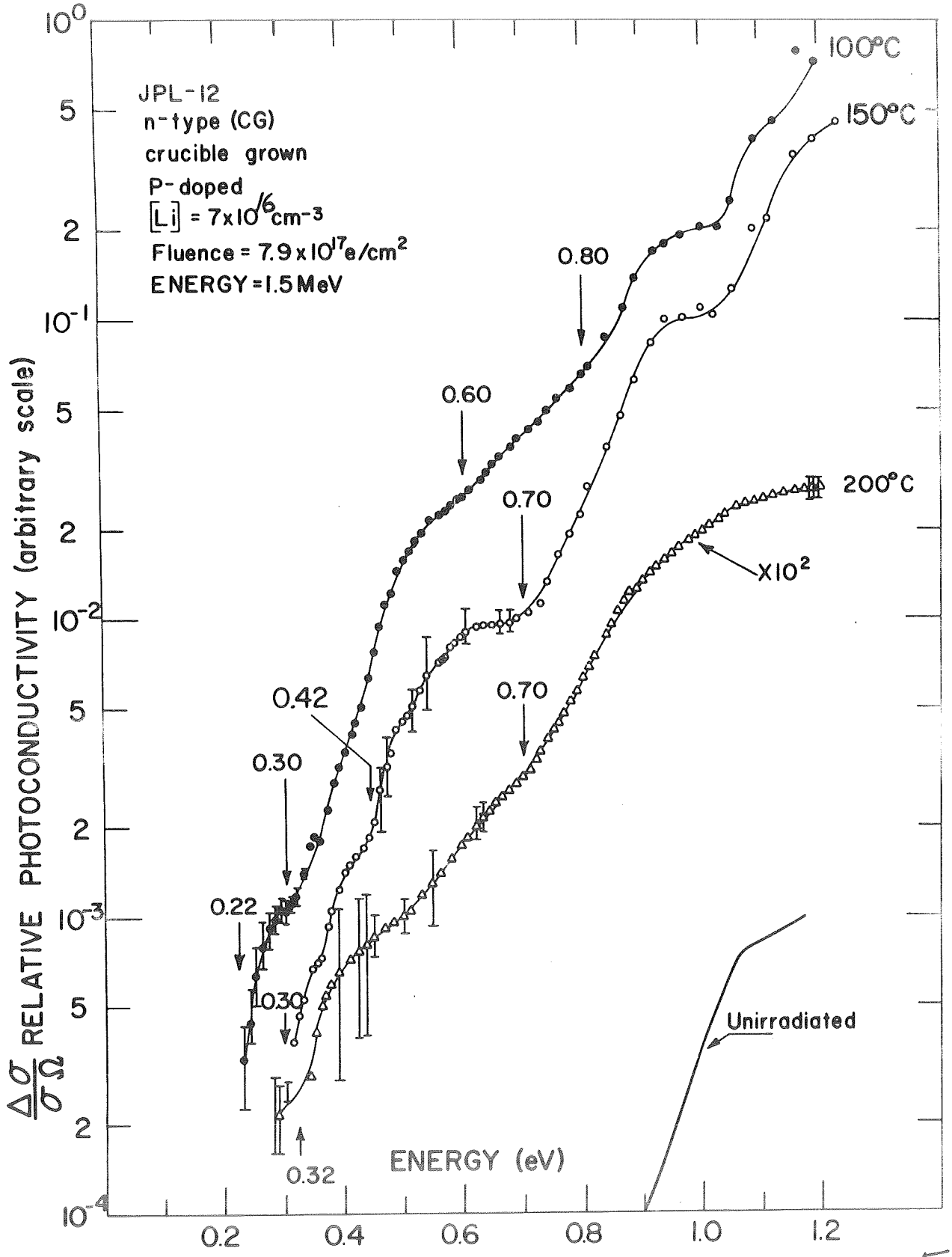
JPL-12
n-type (CG)
crucible grown
P-doped
[Li] = 7x10^16 cm^-3
Fluence = 7.9x10^17 e/cm^2
ENERGY = 1.5 MeV
100°C
150°C
200°C
X10^2
0.80
0.60
0.70
0.42
0.30
0.22
0.30
0.32
0.70
Unirradiated
ENERGY (eV)
RELATIVE PHOTOCONDUCTIVITY (arbitrary scale)
Δσ/σΩ
10^0
5
2
10^-1
5
2
10^-2
5
2
10^-3
5
2
10^-4
0.2
0.4
0.6
0.8
1.0
1.2

Fig. 6.)

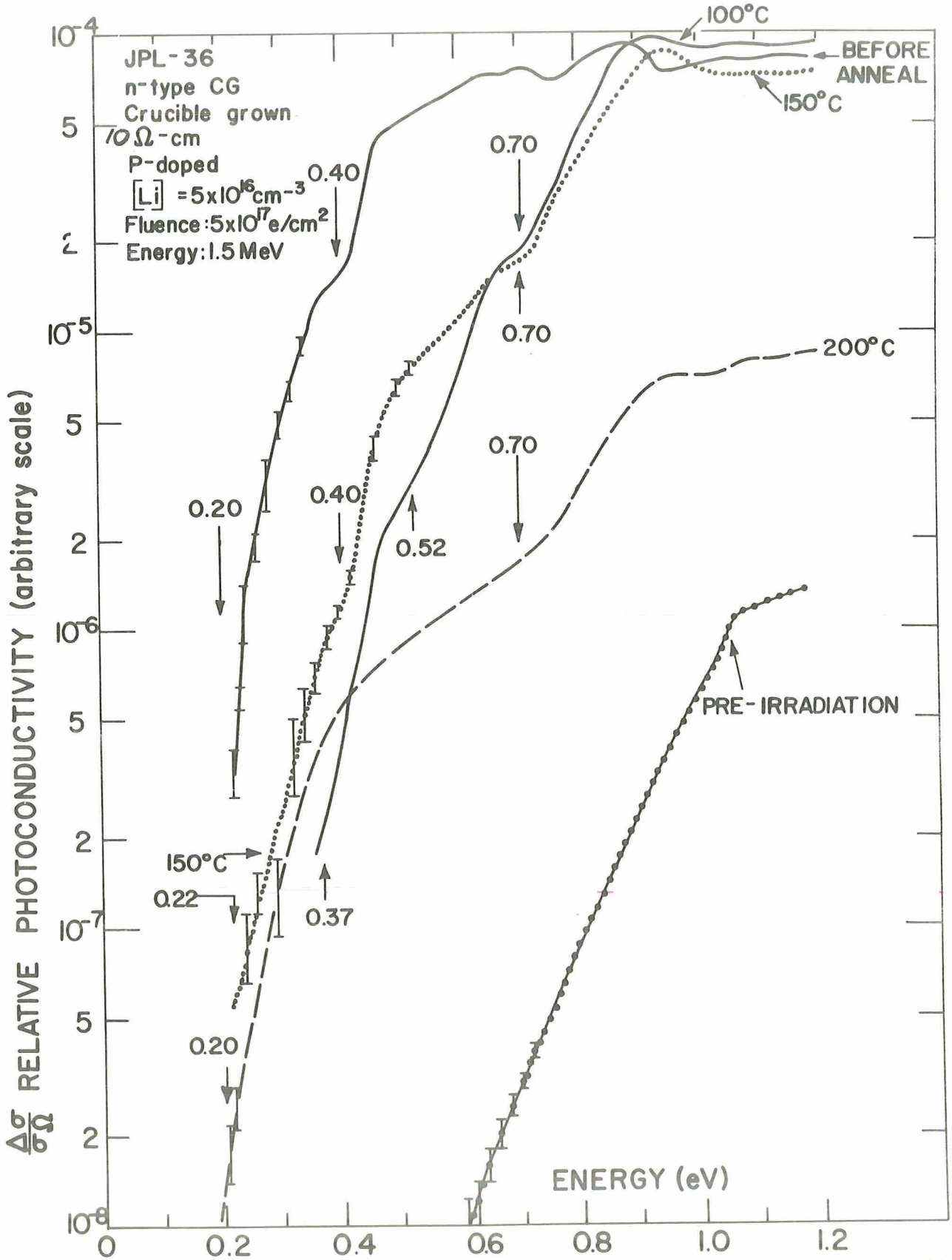
JPL-36
n-type CG
Crucible grown
10 Ω-cm
P-doped
[Li] = 5x10^16 cm^-3
Fluence: 5x10^17 e/cm^2
Energy: 1.5 MeV
100°C
BEFORE ANNEAL
150°C
200°C
PRE-IRRADIATION
0.20
0.40
0.52
0.70
0.22
0.37
ΔσRELATIVE PHOTOCONDUCTIVITY (arbitrary scale)
ENERGY (eV)
10^-4
10^-5
10^-6
10^-7
10^-8
0
0.2
0.4
0.6
0.8
1.0
1.2

Fig. 7.)

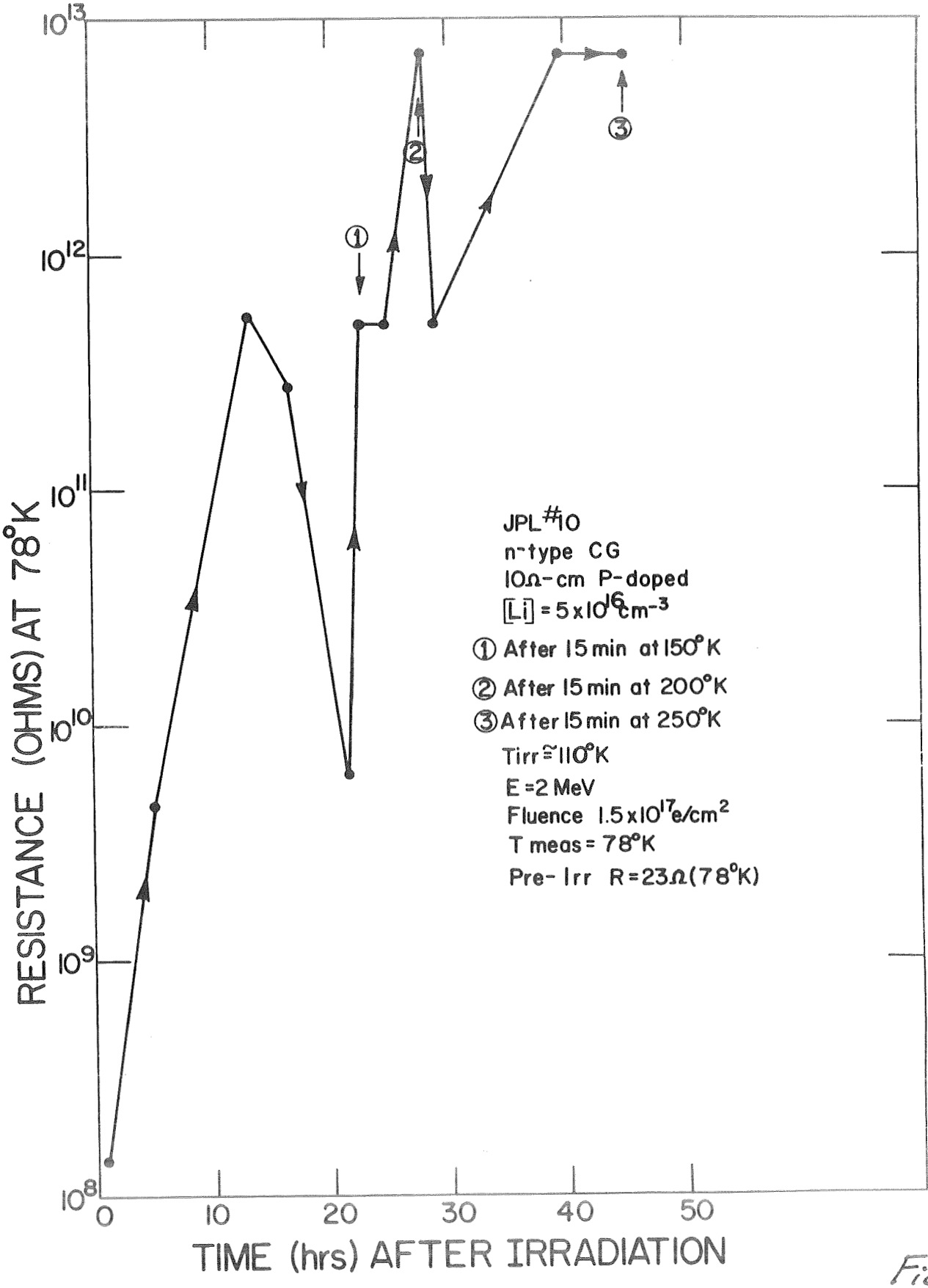
RESISTANCE (OHMS) AT 78°K
TIME (hrs) AFTER IRRADIATION
JPL #10
n-type CG
10Ω-cm P-doped
[Li] = 5x10^16 cm^-3
① After 15 min at 150°K
② After 15 min at 200°K
③ After 15 min at 250°K
Tirr ≅ 110°K
E = 2 MeV
Fluence 1.5x10^17 e/cm^2
T meas = 78°K
Pre-Irr R = 23Ω (78°K)

Fig. 8)

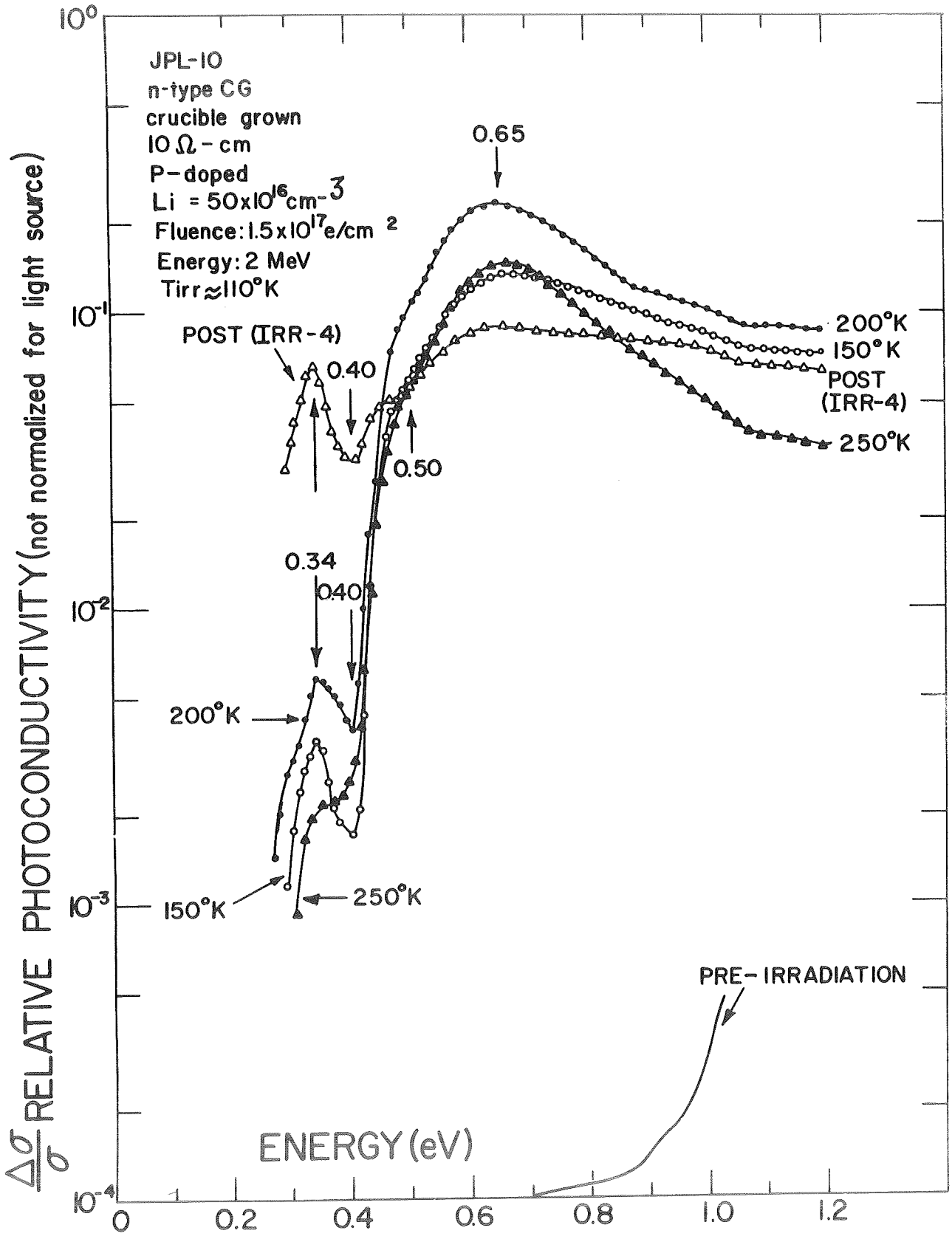
JPL-10
n-type CG
crucible grown
10 Ω - cm
P-doped
Li = 50x10^16 cm^-3
Fluence: 1.5x10^17 e/cm^2
Energy: 2 MeV
Tirr ≈ 110°K
0.65
POST (IRR-4)
0.40
0.50
200°K
150°K
POST (IRR-4)
250°K
0.34
0.40
200°K
150°K
250°K
PRE-IRRADIATION
ENERGY (eV)
Δσ/σ RELATIVE PHOTOCONDUCTIVITY (not normalized for light source)
10^0
10^-1
10^-2
10^-3
10^-4
0
0.2
0.4
0.6
0.8
1.0
1.2

Fig. 9.)

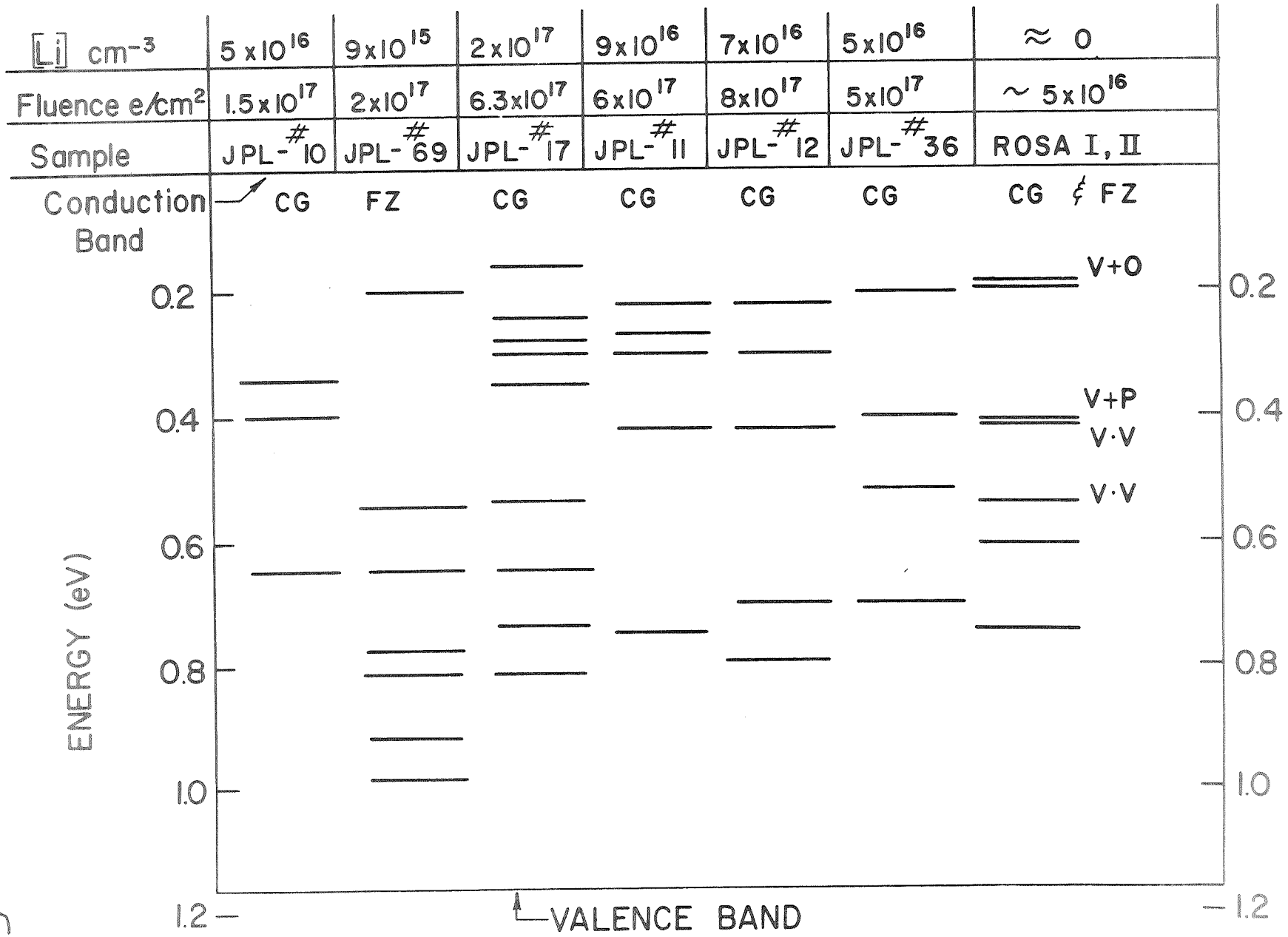
[Li] cm⁻³
5x10¹⁶
9x10¹⁵
2x10¹⁷
9x10¹⁶
7x10¹⁶
5x10¹⁶
≈ 0
Fluence e/cm²
1.5x10¹⁷
2x10¹⁷
6.3x10¹⁷
6x10¹⁷
8x10¹⁷
5x10¹⁷
~ 5x10¹⁶
Sample
JPL-#10
JPL-#69
JPL-#17
JPL-#11
JPL-#12
JPL-#36
ROSA I, II
Conduction Band
CG
FZ
CG
CG
CG
CG
CG & FZ
V+O
V+P
V·V
V·V
ENERGY (eV)
0.2
0.4
0.6
0.8
1.0
1.2
VALENCE BAND

Fig. 1(a)